

A Comprehensive Compressible Injection Model for High Pressure Gaseous Fuel Injectors

Helge von Helldorff, Gerald J Micklow

Dept. Mechanical and Aerospace Engineering
Florida Institute of Technology
Melbourne, FL 32901, USA
hvonhelldorf2008@fit.edu

Abstract— A comprehensive injection model for compressible gas injection to predict the injection velocity and mass flow rate under time-varying pressure ratios was developed, compared to literature data and implemented in KIVA-3V. The model accounts for compressibility effects on the injection gas density and viscosity, variation of the incompressible discharge coefficient with Reynold's Number, as well as a compressible correction to the discharge coefficient. In the presented case, compressible variation of density and viscosity are implemented through empirical relationships for hydrogen. Similar expressions can easily be introduced for alternate gaseous injection media.

For an internal combustion direct injection applications with injection pressures and temperatures of 40 atm and 300K respectively, the effect of the compressibility results in a density reduction of about 10% and marks the most significant factor for high pressure injection flow rate. At these conditions, pressure effects on the viscosity of the hydrogen are nearly negligible, resulting only in a 0.5% increase in viscosity.

The incompressible contribution to the discharge coefficient causes a significant drop in flow rate at low Reynold's Numbers due to the increasing viscous effects. The compressible correction to the discharge coefficient to account for force defects, i.e. pressure drops resulting from high velocity flows at the nozzle exit, increases the discharge coefficient by roughly 10% in the choked flow regime. However, as the discharge coefficient approaches unity, the continuing reduction in density due to the compressibility factor starts to outweigh this force defect contribution and results in a decrease in the ratio of real versus ideal mass flow rate at high Reynold's Numbers.

Keywords— compressible, gaseous, injection, KIVA, discharge coefficient, nozzle

I. INTRODUCTION

Increasingly stringent requirements for efficiency for internal combustion engines and emissions control are requiring the development of ever more sophisticated combustion strategies. In recent years, research of advanced multi-fuel concepts such as Diesel-CNG and other combinations of gaseous and liquid fuels has increased, although practical applications are still rare on the commercial market. Similar to liquid fuels, which have evolved from carburetion to direct injection being almost exclusively used for automotive applications, so is the application of gaseous fuels evolving from ingestion into the air intake to direct injection.

The KIVA code set has been a defining program in the establishment of the modelling of fuel sprays and simulation of internal combustion engines [1]. In a previous

publication, it has been shown that gaseous fuels may also be introduced into the computational domain using this Lagrangian method with only minor changes and corrections to the original KIVA code, similar to the approach proposed by Hessel [2]. It was found that a mesh size on the order of the radius of the injector nozzle is sufficient to predict the macroscopic characteristics of the jet, such as penetration distance and jet plume angle adequately well [3]. This methodology allows for a significant reduction in computational time compared to the explicit modelling of the internal flows of the injector, which is generally computationally cost prohibitive for engineering applications such as extensive parametric studies.

This model utilized mass flow rate and injection velocity as input variables, which is numerically the simplest methodology of describing the injection process. At this point, a significant disconnect between the experimental and computational approach exists, as experimentally these quantities are difficult to assess and generally not reported in many experimental studies, which instead rely on the experimentally easily obtainable pressure differential across the nozzle to describe the injection conditions.

Previously, Micklow et. al. [4] extended the capabilities of the KIVA3V code set by basing the injection parameters, i.e. injection velocity, mass flow rate, particle size etc. solely on the injection pressure ratio and reservoir gas state. The injection velocity is updated at every time step and the corresponding mass flow for the time step is found simply through the application of Bernoulli's equation and the continuity equation.

$$v_{inj} = \sqrt{\frac{2(P_0 - P_{cyl})}{\rho_{liq}}} \quad (1)$$

$$\dot{m} = C_d * A * \rho_{liq} * v_{inj} \quad (2)$$

Since the previous model by Micklow et. al. is only valid for liquid, incompressible fuel sprays, a further extension is required for compressible gaseous injections. This compressible model must include compressibility effects along the nozzle geometry, compressibility effects on the gas characteristics such as density and viscosity, as well as compressibility effects on the geometry-based discharge coefficient. To account for these effects, a comprehensive compressible 1-D model was created to predict the injection velocity and mass flowrate under the conditions of a time-varying pressure ratio in order to negate the need for extensive experimental data at various pressure ratios. This comprehensive model represents a combination of previously established sub models addressing each of the aspects described above.

II. COMPUTATIONAL MODEL

A. Compressible Discharge Coefficient

Borrowing from Jobson [5], who presented an analytical investigation of the effects of compressibility on flow through orifices and nozzles, the following model was amended and discretized for utilization within the KIVA environment. The following expressions for injection velocity and mass flow rate are convenient, as they only require prior knowledge of the injection reservoir quantities, with the exception of the pressure ratio across the nozzle, r , which requires the experimentally easily obtainable in-cylinder pressure.

$$v_{inj} = \frac{K_N}{r^{1/\gamma}} \sqrt{\frac{P_0}{\rho_0}} \quad (3)$$

$$\dot{m} = C_d K_N A \sqrt{P_0 \rho_0} \quad (4)$$

$$K_N \equiv \sqrt{\frac{2\gamma}{\gamma-1} r^{(2/\gamma)} \left(1 - r^{(\frac{\gamma-1}{\gamma})}\right)} \quad (5)$$

For choked flow, the analytical model further simplifies, as the critical pressure ratio remains constant. However, as the expressions for K_N , u and \dot{m} remain valid, explicit implementation of these formulas is not necessary, as long as the pressure ratio variable is limited to the critical pressure ratio.

$$r_c = \left(\frac{2}{\gamma+1}\right)^{\frac{\gamma}{\gamma-1}} \quad (6)$$

$$K_N = \sqrt{\gamma \left(\frac{2}{\gamma+1}\right)^{\frac{\gamma+1}{\gamma-1}}} \quad (7)$$

$$v_{inj,c} = \frac{K_N}{r_c^{1/\gamma}} \sqrt{\frac{P_0}{\rho_0}} \quad (8)$$

$$\dot{m} = C_d K_N A \sqrt{P_0 \rho_0} \quad (9)$$

It should be noted that the specific heats at constant pressure and constant volume differ greatly with temperature and to a lesser degree pressure. However, since only the ratio of the specific heat ratio is used in this formulation, pressure effects are effectively negligible. Since the injection temperature remains within the low temperature regime, the assumption of constant specific heat ratios remains valid.

The only remaining unknown is the discharge coefficient C_d . Jobson introduced a compressible correction to be applied to a previously determined incompressible discharge coefficient, $C_{d,i}$, by calculating the force defect arising from the increase of kinetic energy at the expense of pressure energy as the flow exits the nozzle. This force defect results in a non-uniform pressure distribution at the nozzle exit. This reduced pressure at the nozzle exit thus causes an increase in flow rate as the pressure difference across the nozzle is increased. For clarity, a visual representation of this force defect taken from Jobson [5] is shown in Fig. 1.

The force defect enters the expression for the discharge coefficient in the form of a force defect coefficient, f_i , which is related to the incompressible discharge coefficient $C_{d,i}$.

$$f_i = \frac{1}{C_{d,i}} - \frac{1}{2C_{d,i}^2} \quad (10)$$

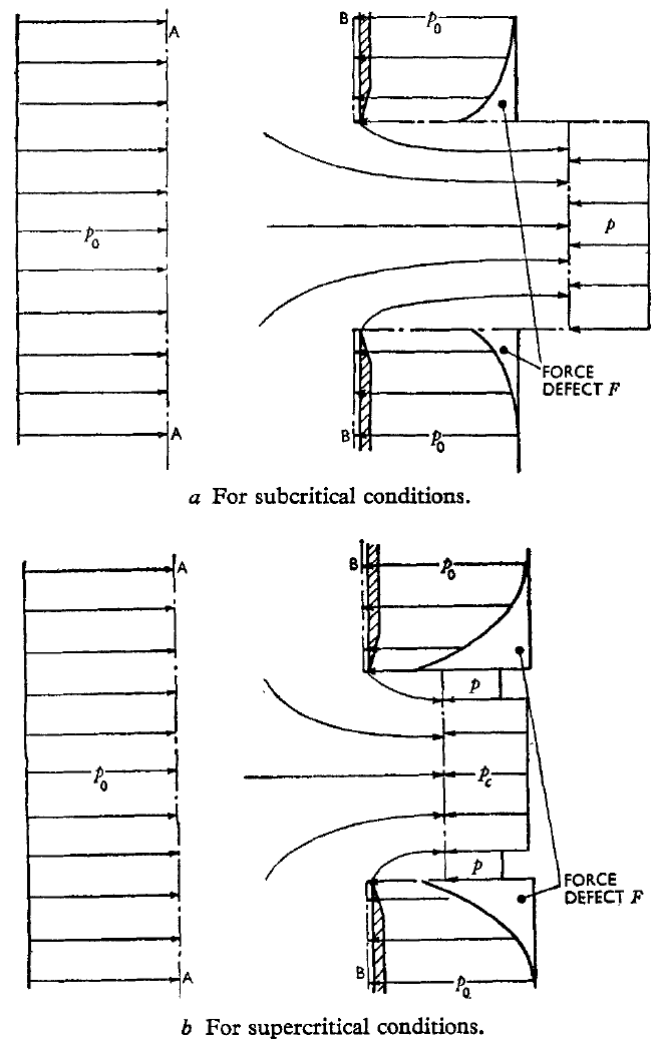


Fig. 1: Visualization of the Force Defect described by Jobson [5]

It should be pointed out that this expression presented by Jobson includes a typographical error. The corrected equation is provided here, where the originally neglected power 2 is highlighted by arrows.

$$C_d = \frac{1}{2f_i r_c^{1/\gamma}} \left[\left\{ 1 + \frac{(r_c-r)r_c^{1/\gamma}}{K_N^2} \right\} - \sqrt{\left\{ \left(1 + \frac{(r_c-r)r_c^{1/\gamma}}{K_N^2} \right)^{-2} - \left(\frac{(2r_c^{1/\gamma})^2 (1-r)f_i}{K_N^2} \right) \right\}} \right] \quad (11)$$

The force defect, as derived by Jobson, assumes that the compressible effects only take place at the nozzle and do not propagate upstream of the nozzle. The flow upstream of the nozzle is thus treated as incompressible. Bragg [6] pointed out that this leads to unrealistic results if the incompressible discharge coefficient is larger than 0.7. Accounting for the compressibility effects upstream of the nozzle, Bragg

introduced the Modified Jobson's Method, which calculates a compressible correction to the force defect coefficient.

As the equations of the Modified Jobson's Method cannot be closed, iterative methods must be utilized to solve the equations to determine the compressible discharge coefficient. It was found that using such iterative methods was in some cases sensitive to the initial guess made for C_d , especially when the first guess was taken as unity or close to unity. However, the incompressible discharge coefficient provided a convenient first guess that was suitable for the entire range of pressure ratios investigated here.

For the subcritical case, the following three equations are solved iteratively. First, the discharge coefficient is guessed to find r_n , which represents the pressure ratio of a hypothetical condition at the edge of the nozzle plane, and used to further calculate the compressible force defect coefficient and finally the compressible discharge coefficient.

$$r_n^{2/\gamma} (1 - r_n^{(\gamma-1)/\gamma}) = k^2 C_d^2 r_a^{2/\gamma} (1 - r_a^{(\gamma-1)/\gamma}) \quad (11)$$

$$\frac{f}{f_i} = \frac{2}{r_n^{1/\gamma}} - \frac{(\gamma-1)(1-r_n)}{\gamma r_a^{2/\gamma} (1-r_a^{(\gamma-1)/\gamma})} \quad (12)$$

$$C_d = \frac{1 - \sqrt{1 - \frac{2f(\gamma-1)(1-r_a)}{\gamma(1-r_a^{(\gamma-1)/\gamma})}}}{2f r_a^{1/\gamma}} \quad (13)$$

The supercritical case is solved analogously, except that the nozzle pressure ratio, r_a is replaced by the critical pressure ratio.

$$r_n^{2/\gamma} (1 - r_n^{(\gamma-1)/\gamma}) = k^2 C_d^2 r_a^{2/\gamma} (1 - r_c^{(\gamma-1)/\gamma}) \quad (14)$$

$$r_c = \left(\frac{2}{\gamma+1}\right)^{\frac{\gamma}{\gamma-1}} \quad (15)$$

$$\frac{f}{f_i} = \frac{2}{r_n^{1/\gamma}} - \frac{(\gamma-1)(1-r_n)}{\gamma r_a^{2/\gamma} (1-r_a^{(\gamma-1)/\gamma})} \quad (16)$$

$$C_d = \frac{1 + \frac{r_c - r_a}{\gamma r_c} - \sqrt{\left(1 + \frac{r_c - r_a}{\gamma r_c}\right)^2 - 2f \frac{\gamma+1}{\gamma} (1-r_a)}}{2f r_c^{1/\gamma}} \quad (17)$$

The constant k in this model represents a geometry dependent factor for each flow nozzle that is otherwise uninfluenced by location within the nozzle nor by the flow conditions, and can thus be viewed as the geometry-only dependent part of the discharge coefficient. For Borda-Mouth Pieces $k=0$, and for smooth converging nozzles $k=1$, in the limiting extreme cases. For the incompressible case with constant incompressible discharge coefficient, Bragg related this parameter, k , to the incompressible force defect coefficient such that $k^2 = 2f_i$, where f_i is a function of $C_{d,i}$. However, in this model, the incompressible discharge coefficient is taken to be variable and dependent on Reynold's Number. For that reason, k is treated as a simple input variable to the model that requires experimental validation with each nozzle geometry modelled. It is taken as unity for comparability of the results presented below.

B. Incompressible Discharge Coefficient

Similar to the compressible discharge coefficient, which varies with flow conditions, so does the incompressible discharge coefficient vary. While treating the discharge coefficient as a constant is common practice for manual

calculations over a limited range of flow conditions, the variations become significant if the range of flow conditions is wide.

Despite the difficulties in comparing discharge coefficients due to the strong influences of the specific nozzle or orifice geometry, numerous empirical relationships have been proposed to predict discharge coefficients. Most commonly, such empirical expressions are functions of Reynold's Number. Additionally, geometric factors such as the ratio of throat to pipe diameter, as in the model presented by Miller [7]. Quing et. al. further present multiple expressions for discharge coefficient for both subcritical and critical flows, and relations for the effects of length-to-width ratio and recess ratio of the injector [8].

Especially at low Reynold's numbers, it can be seen that the discharge coefficient significantly drops compared to the relatively constant behavior as Reynold's Numbers become large. Micklow et. al. [4] presented two such empirical relationships for the discharge coefficient of cylindrical and conical nozzles for incompressible flow that are purely dependent of Reynold's Number.

$$\text{For Cylindrical Nozzles: } C_{d,i} = 0.91 - 8.49/Re^{0.5} \quad (18a)$$

$$\text{For Conical Nozzles: } C_{d,i} = 0.96 - 10.17/Re^{0.5} \quad (18b)$$

For this model, the expression for conical nozzles by Micklow et. al. is utilized to determine the incompressible discharge coefficient and provide closure to the Modified Jobson's Method. This relatively simplistic model only dependent on Reynold's number was chosen to minimize the number of tuning constants present in the overall model, leaving the geometric factor k as the only input variable to the nozzle geometry.

C. Compressibility Effect on Viscosity

Since the incompressible discharge coefficient is a function of Reynold's number, which in turns requires knowledge of the viscosity, an empirical model was used to define the viscosity of the injection gases at the various injection temperatures and pressure. While viscosity is primarily a function of temperature, at very high pressures viscosity becomes dependent on pressure as well.

At moderate pressures, the viscosity of hydrogen is dependent only on temperature. For the temperature range expected for any automotive direct injection process, $5 \leq T_R \leq 75$, Stiel et. al. [9] found the following empirical relationship, where μ^* is the temperature dependent viscosity in centipoise at moderate pressures. The reduced quantities for temperature, pressure and density are defined as:

$$\mu^*(T) = 208 * 10^{-5} T_R^{0.65} \quad (19)$$

$$T_R = \frac{T}{T_c} \quad \text{where } T_c = 33.3 \text{ K} \quad (20)$$

$$P_R = \frac{P}{P_c} \quad \text{where } P_c = 12.8 \text{ atm} \quad (21)$$

$$\rho_R = \frac{\rho}{\rho_c} \quad \text{where } \rho_c = 0.0310 \frac{\text{g}}{\text{cm}^3} \quad (22)$$

For high pressures, Stiel presents data for a pressure correction to the solely temperature dependent expression in the form of a differential viscosity, $\Delta\mu(\rho_R) = \mu(T, P) - \mu^*(T_R)$, but unfortunately does not provide any empirical relationship for the presented data and curve fit. This data was used to create an empirical expression for $\Delta\mu(\rho_R)$.

For $0 \leq \rho_R \leq 1.5$ the differential viscosity is estimated as

$$\Delta\mu(\rho_R) = 17.859 * (e^{1.8986*\rho_R} - 1) \quad (22)$$

and for $\rho_R > 1.5$, the following 6th order polynomial expression was found.

$$\Delta\mu(\rho_R) = \{3000.5 * \rho_R^6 - 27097 * \rho_R^5 + 99144 * \rho_R^4 - 186538 * r\rho_R^3 + 188556 * \rho_R^2 - 95545 * \rho_R + 18604\} * 10^{-5} \quad (23)$$

Such that $\mu(T, P) = \mu^*(T) + \Delta\mu(\rho_R)$ gives the temperature and pressure dependent viscosity in centipoise. These expressions found through regression analysis are accurate within the readability limits of the data presented by Stiel, as represented in Fig. 2.

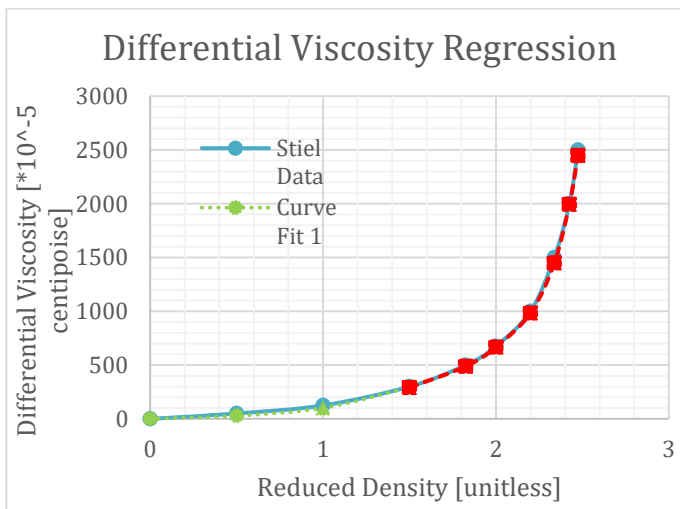


Fig. 2: Pressure-dependent differential viscosity regression

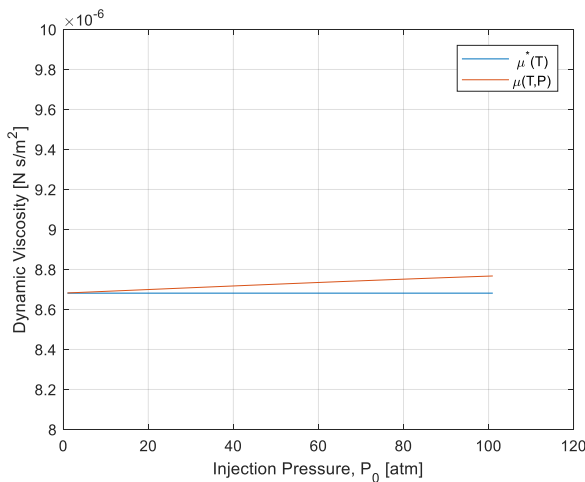


Fig. 3: Effect of Pressure on dynamic viscosity

The reservoir total pressure, P_0 , and reservoir total temperature, T_0 , are set as input variables to the combined model, allowing for the calculation of the reservoir density, ρ_0 . In many cases, gaseous injectors are designed to operate at choked conditions in order to provide a constant injection profile. For compression ignition engines with compression ratios on the order of 15-20, this means that the injection pressure must be on the order of 30-40 atm in order to maintain the choked flow. Within this pressure range, it can be seen that viscosity increases nearly linearly with pressure, while μ^* remains constant since the injection velocity is held

constant at 300K. As shown in Fig. 3, pressure effects on dynamic viscosity are mostly negligible accounting only for about 0.5% of the value of dynamic viscosity. The pressure correction for viscosity was, however, still implemented for flexibility of the presented model to be used for higher pressure applications as well.

D. Compressibility Effect on Density

At these pressures on the order of 40 atm, real gas effects become significant such that the compressibility factor must be accounted for in the calculations. Countless empirical models exist for various gases to predict the compressibility factor, Z . The compressibility factor Z is commonly found in many fluid dynamics textbooks in the form of generalized plots as a function of reduced temperature and pressure, i.e. the ratio of actual temperature and pressure over their respective critical values. While these plots provide a convenient method for hand calculations, they do not lend themselves to be easily implemented in computer programs. Alternatively, generalized algebraic expressions applicable to various substances exist, which are much more easily implemented in computer codes. The Redlich-Kwong model [10], the Peng-Robinson model [11] and the Lee Kesler model [12] are among the most well-known such models. In this model, an expression specifically applicable to hydrogen was implemented. The model proposed by Lemmon et. al. [13] was utilized here for its simple implementation, which does not require iterative processes, and its high accuracy of 0.01% error within the pressure and temperature ranges expected for gaseous fuel injection into CI engines.

$$Z(P, T) = \frac{P}{\rho R T} = 1 + \sum_{i=1}^9 \left\{ a_i \left(\frac{100K}{T} \right)^{b_i} \left(\frac{P}{1MPa} \right)^{c_i} \right\} \quad (24)$$

TABLE I. COMPRESSIBILITY MODEL COEFFICIENTS

i	a_i	b_i	c_i
1	0.058 884 60	1.325	1.0
2	-0.061 361 11	1.87	1.0
3	-0.002 650 473	2.5	2.0
4	0.002 731 125	2.8	2.0
5	0.001 802 374	2.938	2.42
6	-0.001 150 707	3.13	2.63
7	0.958 852 8 $\times 10^{-4}$	3.37	3.0
8	-0.110 904 0 $\times 10^{-6}$	3.75	4.0
9	0.126 440 3 $\times 10^{-9}$	4.0	5.0

As expected, the compressibility factor Z depicted in Fig. 4 is nearly proportional to pressure and changes only slightly more than linearly with increasing injection pressure at constant injection temperature, owing to the simplistic atomic structure of diatomic hydrogen. For hydrogen at 40 atm, the resulting decrease in density is nearly 10% compared to ideal gas calculations.

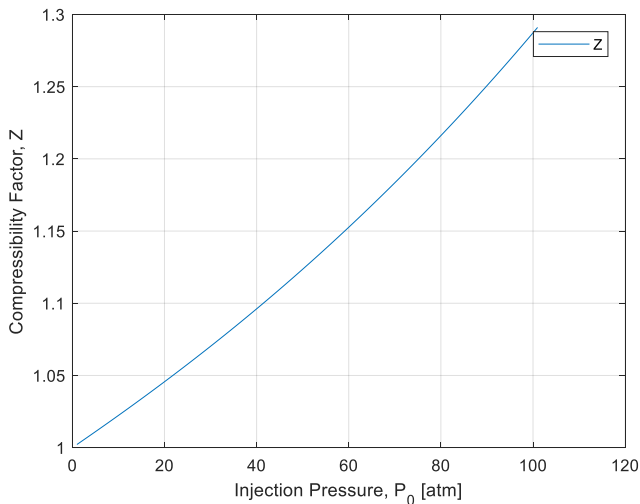


Fig. 4: Compressibility Factor vs. Pressure

E. Implementation in KIVA-3V

The presented model was developed in Matlab to produce values for the injection velocity, mass flow rate and discharge coefficient over a wide range of pressure ratios. Finally, the complete model was implemented in KIVA-3V release 2 such that at each time step the average mass flow rate between the current time step t and the previous time step $t-1$ was used to determine the mass to be introduced into the computational domain.

$$tm_{inj}^t = tm_{inj}^{t-1} + (\dot{m}^t + \dot{m}^{t-1}) * dt/2 \quad (25)$$

The KIVA implementation was then back-checked against the Matlab model at various arbitrary pressure ratios to ensure proper functionality.

III. RESULTS

All results presented here were obtained by implementing the combined models described above in Matlab and solving for injection pressures, P_0 , ranging from 1 to 80 atm, while keeping the injection temperature, T_0 , constant at 300K and keeping the cylinder (i.e. receiving volume) pressure constant at 1 atm. The flow-independent geometry factor k is taken to be unity for this comparison.

Fig. 5 depicts the behavior of mass flow rate and injection velocity compared to the pressure ratio across the nozzle. It can be seen that injection velocity rises very quickly as the reservoir pressure is increase (i.e. the pressure ratio is decreased). As the nozzle gets choked at the critical pressure ratio, the velocity profile levels out. However, a slight positive slope remains due the effect compressibility on the density of the injection gas. If plotted directly versus the reservoir pressure, the mass flow rate displays a nearly entirely linear behavior with injection pressure. This is due to the fact that the mass flow rate is driven by the changes in density with increasing pressure. Thus, even when the nozzle is choked the density increases linearly, owing to the near linear behavior of compressibility factor, Z .

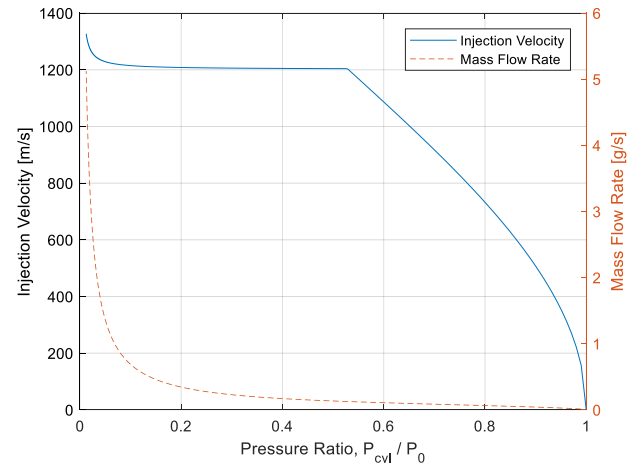


Fig. 5: Injection Velocity and mass flow rate vs pressure ratio

Fig. 6 depicts the incompressible discharge coefficient and the compressibility-corrected discharge coefficient. As, expected the influence of the compressibility correction is small when the pressure ratio is near unity and increases as compressible effects become more prevalent when the difference in pressure is large. Notably, the incompressible discharge coefficient is quite low but rises quickly at pressure ratios near unity.

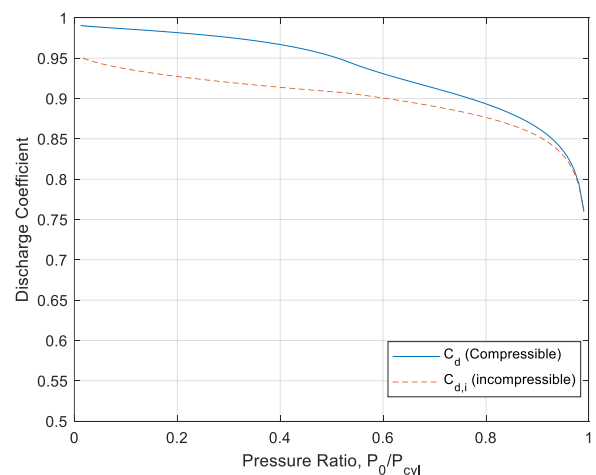


Fig. 6: Discharge coefficient vs pressure ratio

Discharge coefficients from various experimental studies are notoriously difficult to compare due to the strong dependence of discharge coefficient on even minute geometrical differences. Fig. 7 compares the ratio of computed mass flow rate to ideal mass flow rate with literature results presented by Nagao et. al. [14] and depicted in Fig. 8. The ideal mass flow rate here is computed identically to the analysis by Nagao (see equation 26). It should be noted that the computational results presented by Nagao only represent the effect of the compressibility factor Z and does not incorporate additional compressible effects occurring inside the nozzle such as the force defect described by Jobson nor any other real world effects, such as viscous contributions, which become significant at low Reynold's Numbers. It is thus expected that the discharge coefficient presented by this model are overall lower, as these real flow contributions to the discharge coefficient are neglected by these literature results.

$$\dot{m}_{ideal} = \frac{AP_0}{\sqrt{R_0T_0}} \left\{ \gamma \left(\frac{2}{\gamma+1} \right)^{\frac{\gamma+1}{\gamma-1}} \right\}^{1/2} \quad (26)$$

It can be seen that the compressibility factor, Z, has by far the most significant effect on the mass flow rate. The effect of viscosity, and especially viscosity variation with pressure, on the other hand is mostly insignificant. Further, the model presented here predicts a significantly steeper drop of discharge coefficient at low Reynold's Number, which is due to the incorporation of the reduction of incompressible discharge coefficient at low Reynold's Number. This sharp drop in discharge coefficient is similarly described by other publications of experimental investigations such as Moroika et. al. [15] and Belforte [16]. However, this low Reynold's Number flow regime is expected to be rarely encountered in most internal combustion injection applications. The maximum value of discharge coefficient, occurring at Reynold's Numbers around 10^5 matches the literature data well for the presented case of smooth converging nozzle with geometric tuning constant k equal to unity. In cases where the nozzle significantly departs from the assumption of the smooth converging nozzle, this tuning constant provides a convenient method for adjustment to the model based on experimental data. The reduction in discharge coefficient with increasing Reynold's Number due to compressibility effects of the reservoir gas is qualitatively well-captured. Again, the introduction of additional compressibility effects near the nozzle reduce the quantitative values in this regime.

It should be noted, that the discharge coefficient as defined in Fig. 7 and Fig. 8 includes the effect of the compressibility factor, while the discharge coefficient defined within the Modified Jobson's Method does not include the compressibility factor as these effects are already incorporated in the density calculation for the model presented in this paper.

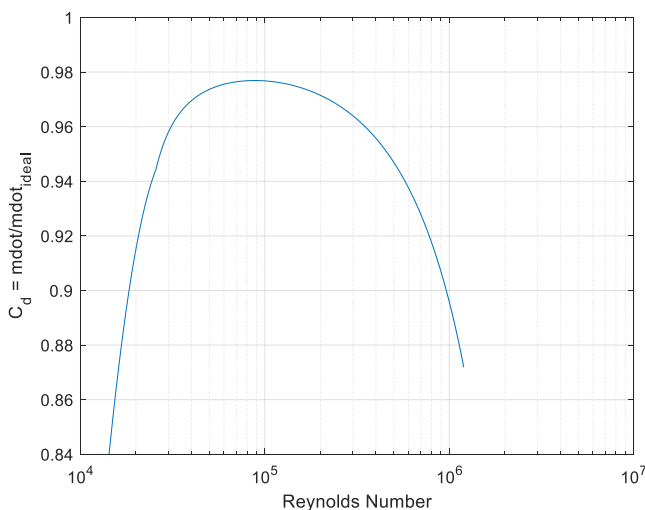


Fig. 7: Ratio of Computed mass flow rate to ideal mass flow rate

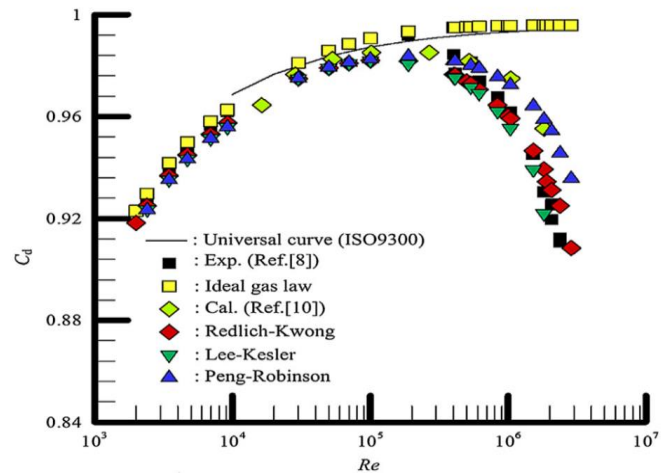


Fig. 8: Literature results for ratio of computed mass flow rate to ideal mass flow rate [14]

IV. CONCLUSIONS

A comprehensive 1-D model to describe the injection mass flow rate and injection velocity of a compressible gas is presented. The model was implemented in KIVA 3V release 2 to predict these quantities for a fixed injection reservoir pressure into a volume with time-varying pressures. The compressible injection model was based on the analytically derived Jobson's Method and extended to account for various compressibility effects.

The model incorporates the compressibility factor, Z, which for this model was implemented for hydrogen. The compressibility factor was shown to have significant effects on the injection mass flow rate and velocity due to the 10% reduction in density for pressures of 40 atm.

An empirical expression for the pressure variation of hydrogen viscosity was developed and implemented. Viscous variations with pressure were found to be nearly negligible at pressures of 40 atm and 300K reservoir temperature.

The incompressible discharge coefficient was modelled similarly to a previously developed incompressible injection model and in particular describes the significant drop in flow rate at low Reynold's Numbers due to the increasing significance of viscous effects in this flow regime.

The incompressible discharge coefficient is modified through application of the Modified Jobson's Method to incorporate compressible pressure drops at the nozzle exit arising from the high exit jet velocity. The compressible correction to the discharge coefficient increases the discharge coefficient by roughly 10% in the choked flow regime while approaching zero as the pressure ratio approaches unity.

The peak discharge coefficient of about 0.98 occurs at Reynold's Numbers of 10^5 for the case of a smooth converging nozzle, which is on the same order as suggested by literature data for ideal nozzles. If the nozzle significantly departs from the smooth, slowly converging nozzle assumption, the flow independent geometry factor, k, in the presented model provides a convenient tuning constant to account for specific nozzle geometries based on experimental data.

V. NOMENCLATURE

A. Variables and constants

v_{inj} = injection velocity

P = pressure

T = Temperature

\dot{m} = mdot = injection mass flow rate

ρ = density

A = nozzle area

C_d = discharge coefficient

γ = specific heat ratio

$r = \frac{P}{P_0}$ = pressure ratio

K_N = mass flow coefficient

f = force defect coefficient

μ = dynamic viscosity

$\Delta\mu$ = differential viscosity accounting for
pressure effects on viscosity

k = geometry dependent constant uninfluenced
by location within the nozzle nor by the flow conditions

Re = Reynold's Number

tm_{inj}^t = total mass injected between t = 0
and current time step

dt = time step

R = universal gas constant

B. Suffixes

c = critical

i = incompressible

0 = total reservoir quantity

liq = liquid

cyl = condition in cylinder/injection receiving volume

n = hypothetical condition at edge of orifice

a = flow conditions on expansion to atmospheric pressure

R = reduced

t = computational time level t

* = only temperature dependent at moderate pressures

Engineering Science and Technology (JMEST), vol. 6, no. 1, pp. 9424-9432, 2019.

- [4] G. J. Micklow, K. Ankem and T. Abdel-Salam, "A Comprehensive Fuel Spray Model for High Pressure Fuel Injectors," in ASME Turbo Expo 2008: Power for Land, Sea, and Air, Berlin, Germany, 2008.
- [5] D. A. Jobson, "On the Flow of a Compressible Fluid through Orifices," Proceedings of the Institution of Mechanical Engineers, vol. 169, no. 1, pp. 767-776, 1955.
- [6] S. L. Bragg, "Effect of Compressibility on the Discharge Coefficient of Orifices and Convergent Nozzles," Journal of Mechanical Engineering Science, vol. 2, no. 1, pp. 35-44, 1960.
- [7] R. W. Miller, Flow Measurement Engineering Handbook, 3rd ed., New York: McGraw-Hill, 1997.
- [8] L. Qing, L. Qinglian and W. Zhenguang, "Research on Gas Discharge Coefficient of Annular Coaxial Orifice," in 43rd AIAA/ASME/SAE/ASEE Joint Propulsion Conference & Exhibit, Cincinnati, OH, 2007.
- [9] L. I. Stiel and G. Thodos, "Viscosity of Hydrogen in the Gaseous and Liquid States for Temperatures up to 5000K," Industrial & Engineering Chemistry Fundamentals, vol. 2, no. 3, pp. 233-237, 1963.
- [10] O. Redlich and J. N. S. Kwong, "On the Thermodynamics of Solutions. V. An Equation of State. Fugacities of Gaseous Solutions," Chemical Reviews, vol. 44, no. 1, p. 233-244, 1949.
- [11] D. Y. Peng and D. B. Robinson, "A New Two-Constant Equation of State," Industrial and Engineering Chemistry: Fundamentals, vol. 15, p. 59-64, 1976.
- [12] I. Lee and M. G. Kesler, "A Generalized Thermodynamic Correlation Based on Three-Parameter Corresponding States," AIChE Journal, vol. 21, no. 3, pp. 510-527, 1975.
- [13] E. W. Lemmon, M. L. Huber and J. W. Leachman, "Revised Standardized Equation for Hydrogen Gas Densities for Fuel Consumption Applications," Journal of Research of the National Institute of Standards and Technology, vol. 113, no. 6, pp. 341-350, 2008.
- [14] J. Nagao, S. Matsuo, S. Suetsu, T. Setoguchi and H. D. Kim, "Characteristics of high Reynolds number flow in a critical nozzle," International Journal of Hydrogen Energy, vol. 38, pp. 9043-9051, 2013.
- [15] T. Morioka, S. Nakao and M. Ishibashi, "Characteristics of Critical Nozzle Flow Meter for Measuring High-Pressure Hydrogen Gas," in Transactions of the Japan Society of Mechanical Engineers (Part B), 2011.
- [16] G. Belforte, T. Raparelli, V. Viktorov and A. Trivella, "Discharge coefficients of orifice-type restrictor for aerostatic bearings," Tribology International, vol. 40, p. 512-521, 2007.

VI. REFERENCES

- [1] Amsden, P. O'Rourke and T. Butler, "KIVA-II: A Computer Program for Chemically Reactive Flows with Sprays," Los Alamos Report LA-11560-MS, 1989.
- [2] R. P. Hessel, N. Abani, S. M. Aceves and D. L. Flowers, "Gaseous Fuel Injection Modeling Using a Gaseous Sphere Injection Methodology," in Powertrain & Fluid Systems Conference & Exhibition, Toronto, Canada, 2006.
- [3] H. von Helldorff and G. Micklow, "Gaseous and Liquid Jet Direct Injection Simulations Using KIVA-3V," Journal of Multidisciplinary